Subpicosecond oxygen trapping in the heme pocket of the oxygen sensor FixL observed by time-resolved resonance Raman spectroscopy

Sergei G. Kruglik[†‡§], Audrius Jasaitis[†‡], Klara Hola[†‡], Taku Yamashita[†‡], Ursula Liebl[†‡], Jean-Louis Martin[†‡], and Marten H. Vos[†‡¶]

[†]Laboratoire d'Optique et Biosciences, Centre National de la Recherche, Ecole Polytechnique, 91128 Palaiseau Cedex, France; [‡]Institut National de la Santé et de la Recherche Médicale, Unité Mixte de Recherche 696, 91128 Palaiseau, France; and [§]Laboratoire de Biophysique Moléculaire, Cellulaire, et Tissulaire, Centre National de la Recherche Scientifique, Unité Mixte de Recherche 7033, University Pierre & Marie Curie, Genopole Campus 1, Batiment Genavenir 8, 5 Rue Henri Desbrueres, 91030 Evry, France

Edited by William A. Eaton, National Institutes of Health, Bethesda, MD, and approved March 14, 2007 (received for review January 17, 2007)

Dissociation of oxygen from the heme domain of the bacterial oxygen sensor protein FixL constitutes the first step in hypoxia-induced signaling. In the present study, the photodissociation of the heme-O_2 bond was used to synchronize this event, and time-resolved resonance Raman (TR^3) spectroscopy with subpicosecond time resolution was implemented to characterize the heme configuration of the primary photoproduct. TR^3 measurements on heme-oxycomplexes are highly challenging and have not yet been reported. Whereas in all other known six-coordinated heme protein complexes with diatomic ligands, including the oxymyoglobin reported here, heme iron out-of-plane motion (doming) occurs faster than 1 ps after iron–ligand bond breaking; surprisingly, no sizeable doming is observed in the oxycomplex of the *Bradyrhizobium japonicum* FixL sensor domain (FixLH). This assessment is deduced from the absence of the iron–histidine band around 217 cm^{-1} as early as 0.5 ps. We suggest that efficient ultrafast oxygen rebinding to the heme occurs on the femtosecond time scale, thus hindering heme doming. Comparing WT oxy-FixLH, mutant proteins FixLH-R220H and FixLH-R220Q, the respective carbonmonoxy-complexes, and oxymyoglobin, we show that a hydrogen bond of the terminal oxygen atom with the residue in position 220 is responsible for the observed behavior; in WT FixL this residue is arginine, crucially implicated in signal transmission. We propose that the rigid O_2 configuration imposed by this residue, in combination with the hydrophobic and constrained properties of the distal cavity, keep dissociated oxygen in place. These results uncover the origin of the ''oxygen cage'' properties of this oxygen sensor protein.

heme protein | molecular dynamics | ultrafast spectroscopy | vibrational spectroscopy

In many heme proteins, the chemical bond between the heme iron and exogenous molecular oxygen plays an important role in physiological processes, such as oxygen transport/storage [(hemoglobin, myoglobin (Mb)], catalysis (oxidases, NO synthase) and sensing of dioxygen (FixL and Dos). The bacterial oxygen sensor FixL bears a b type heme, like myoglobin bears, but has a relatively low affinity ($\approx$100 μM) for oxygen (1), which makes its oxygenation state a sensitive marker in the physiological range. In FixL, specific binding of oxygen to the heme sensor domain (FixLH) leads to a dramatic decrease in the activity of an associated kinase domain (2), presumably brought about by oxygen-sensitive interactions between the two domains. It has been proposed that a particular arginine residue (R220 in FixL from *Bradyrhizobium japonicum*; Fig. 1) plays an important role, because it undergoes a remarkably substantial conformational change between the O_2-bound steady state (where it is H bonded to the heme-bound O_2) and the deoxy steady-state (where it interacts with heme propionate 7) (3–5).

One way to detect intermediates in the sensing pathway is to synchronize dissociation of ligand from the heme, making use of the photolability of the heme–ligand bond (6). Using femtosecond transient absorption spectroscopy, we observed that excitation of the FixLH–O_2 oxy complex leads to a state with an electronic spectrum of the heme strongly perturbed with respect to that of both steady-state deoxy and oxy complexes and assigned to a perturbed deoxy state. This state was found to decay rapidly ($\approx$5 ps) and efficiently ($\approx$90%) back to the oxy complex, leading to a very low yield of dissociated oxygen after a few tens of picoseconds (7). Thus, despite the low overall oxygen affinity, the heme pocket appears to act as an efficient oxygen trap. Further studies on FixLH mutant proteins indicate that the interaction of R220 with the terminal oxygen atom plays an important role (8, 9).

The steady-state absorption spectra of the oxy and deoxy complexes of FixLH closely resemble those of myoglobin (10) and also the coordination geometries of oxygen, heme, and the proximal histidine residue of both oxy complexes are very similar (3). Yet the reconstructed absorption spectrum of the transient photoproduct of oxy FixLH is close to that of the oxy complex (7), whereas in myoglobin it is very similar to that of the deoxy complex (7). To shed light on structural properties of the photoinduced transient species, in the present work we have investigated, by subpicosecond time-resolved resonance Raman (TR^3) spectroscopy, the initial photoproduct heme state in FixLH–O_2 from *Bradyrhizobium japonicum* and compared it with that of oxymyoglobin, FixLH mutants and their carbonmonoxy complexes.

TR^3 spectroscopy has been successfully used to characterize photodissociated heme–CO, heme–NO, and heme–methionine complexes in various six-coordinated heme proteins on the picosecond time scale (11–20), and these studies clearly indicate that deoxy-like species appear within 1 ps after photoexcitation. However, such studies are extremely challenging for the physiologically relevant ligand oxygen and have not been reported yet, even for the well studied oxygen carriers myoglobin and hemo-

Author contributions: S.G.K., U.L., J.-L.M., and M.H.V. designed research; S.G.K., A.J., K.H., and T.Y. performed research; K.H. and U.L. contributed new reagents/analytic tools; S.G.K. analyzed data; and S.G.K. and M.H.V. wrote the paper.

The authors declare no conflict of interest.

This article is a PNAS Direct Submission.

Abbreviations: 5cHS, five-coordinate high spin; 6cLS, six-coordinate low spin; cw, continuous wave; FixLH, FixL heme domain; RR, resonance Raman; TR^3, time-resolved resonance Raman.

[¶]To whom correspondence should be addressed at the † address. E-mail: marten.vos@polytechnique.edu.

This article contains supporting information online at www.pnas.org/cgi/content/full/0700445104/DC1.

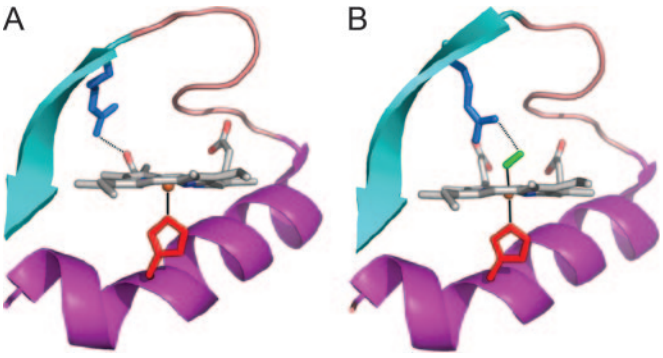

Fig. 1. Crystallographic structures of the ferrous deoxy complex [Protein Data Bank (PDB) ID no. 1LSW; ref. 4] (*A*) and oxycomplex (PDB ID no. 1DP6; ref. 3) (*B*) of FixLH. The residues shown are the proximal histidine (H200, red) and the distal argine (R220, blue). The latter forms a salt bridge with heme propionate 7 in the deoxy form and a hydrogen bond with O_2 (green) in the oxy complex. The figure was prepared using PYMOL.

globin, presumably at least in part because of technical difficulties related to the high autooxidation rate (21), and low photodissociation quantum yield (22). We have developed a time-resolved Raman spectrometer (17, 19, 20, 23) and specific experimental conditions (see *Materials and Methods*) allowing reliable measurements of TR^3 spectra of heme protein oxy complexes with subpicosecond time resolution. In particular, we investigated the low-frequency region around 220 cm^{-1} of the Fe-His band, which is a bench-mark for the appearance of a five-coordinated "domed" (Fe out-of-plane) heme structure (24), as well as the characteristic Raman band shifts in the high-frequency region 1,300–1,700 cm^{-1} of the porphyrin marker bands (25). We discovered that, specifically for WT FixLH, the deoxy-like structure with heme doming does not appear upon dissociation of the oxygen ligand, even at time delays as short as 0.5 ps, indicating that O_2 recombination occurs very rapidly, most probably to a planar heme.

Results

Fig. 2 presents steady-state resonance Raman (RR) and TR^3 spectra of WT ferrous FixLH, in the high-frequency region of the porphyrin marker bands (25). Spectra a, d, and h are ground-state RR spectra of the oxy, CO-bound, and deoxy form respectively, measured with continuous wave (cw) excitation at 441.6 nm. Spectra a and d are consistent with a six-coordinate low-spin (6cLS) heme iron configuration with histidine and a diatomic gaseous molecule as axial ligands, whereas spectrum h is a typical RR spectrum of a five-coordinate high-spin (5cHS) heme with only histidine as an axial ligand, in agreement with literature data (8, 26–28). Spectra b, e, and i also represent the ground-state scattering from these species but with 435-nm excitation by subpicosecond laser pulses in a pump-probe configuration, where the probe pulse arrives before the pump ($\Delta t = -5$ ps). Because of the decreased spectral resolution in the subpicosecond Raman experiments, lines in these spectra are broader than in the steady-state spectra obtained with cw excitation. Nevertheless, the corresponding spectra (a and b, d and e, and h and i) are very similar, thus proving the absence of a perturbing influence of the subpicosecond probe pulse, as well as the absence of any accumulated photoproduct due to the pump pulse with a 1-kHz repetition rate.

Spectra f and g are difference TR^3 spectra obtained after weighted subtraction of the ground-state spectrum (Fig. 2, spectrum e) of FixLH–CO from the measured spectra (data not shown) at $\Delta t = 2$ ps and $\Delta t = 20$ ps, respectively, representing pure scattering from the transient photoproduct species. The procedure

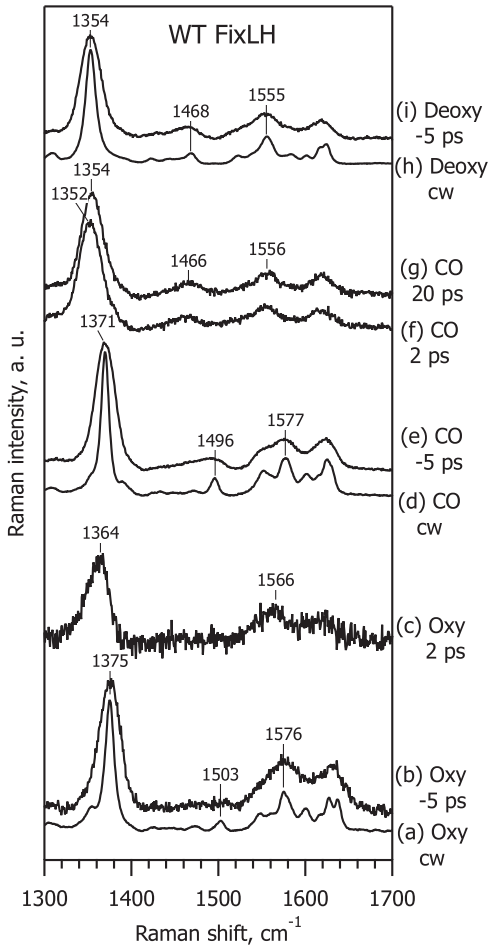

Fig. 2. Steady-state RR and TR^3 spectra in the high-frequency range of ferrous WT FixLH, for the oxy complex (spectra a–c), CO-bound complex (spectra d–g), and deoxy form (spectra h and i). Spectra a, d, and h are ground-state spectra recorded with cw excitation at 441.6 nm. Spectra b, e, and i are ground-state spectra recorded with subpicosecond excitation at 435 nm, when the pump pulse arrived 5 ps after the probe pulse ($\Delta t = -5$ ps). Spectra c, f, and g are difference TR^3 spectra, at $\Delta t = 2$ ps (spectra c and f) and 20 ps (spectrum g).

of TR^3 spectra subtraction is described in detail elsewhere (17, 20, 29). The TR^3 difference spectrum at $\Delta t = 20$ ps (Fig. 2, spectrum g) is very similar to the deoxy spectrum (Fig. 2, spectrum i), and is fully consistent with the efficient photodissociation of the CO axial ligand (7). The ν_4^* band in the $\Delta t = 2$ ps spectrum (~1,352 cm^{-1}, Fig. 2, spectrum f) is slightly low-frequency shifted with respect to $\Delta t = 20$ ps (1,354 cm^{-1}; Fig. 2, spectrum g), presumably because of vibrational heating (14, 20).

In contrast to the FixLH-CO form, the TR^3 spectrum of the FixLH-O_2 photoproduct at $\Delta t = 2$ ps (Fig. 2, spectrum c) differs markedly from the deoxy spectrum (Fig. 2, spectrum i). The spectral differences can be summarized as follows: (*i*) the frequencies of the ν_2^* (≈1,566 cm^{-1}) and ν_4^* (≈1,364 cm^{-1}) bands of the oxy complex photoproduct are far from that of the deoxy form (1,555 cm^{-1} and 1,354 cm^{-1}, respectively); (*ii*) the shape of the ν_4^* band at ≈1,364 cm^{-1} is asymmetrical; and (*iii*) the ν_3 band at ≈1,468 cm^{-1}, typical for a 5cHS deoxy structure, is not observed in the TR^3 difference spectrum of the oxy-photoproduct (Fig. 2, spectrum c), whereas it is well detectable in the spectra of the CO photoproduct (Fig. 2, spectra f and g). These results indicate that a deoxy-like configuration is not readily generated upon photoexcitation of the FixLH–O_2 complex.

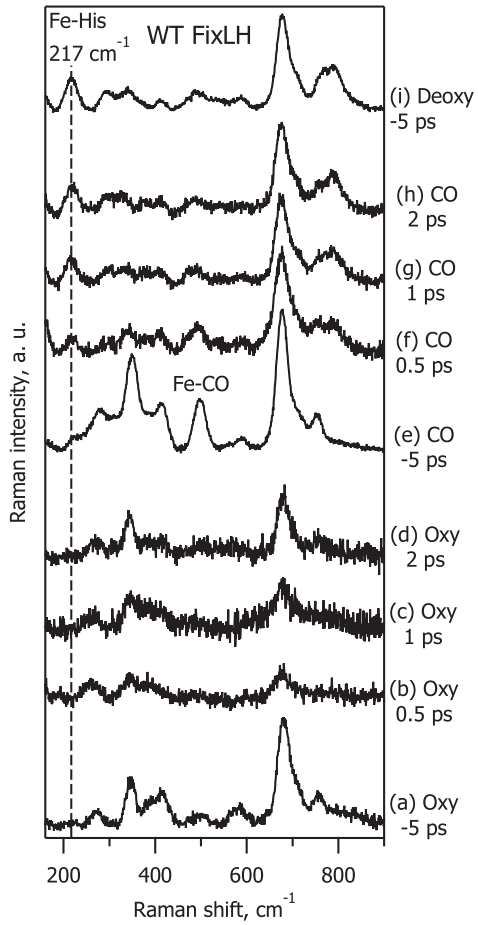

Fig. 3. TR^3 spectra in the low-frequency range of ferrous WT FixLH, for the oxy complex (spectra a–d), CO-bound complex (spectra e–h), and deoxy form (spectrum i). Spectra a, e, and i are ground-state spectra recorded at $\Delta t = -5$ ps. Spectra b–d and f–h are difference spectra at $\Delta t = 0.5$ ps (spectra b and f), 1 ps (spectra c and g) and 2 ps (spectra d and h).

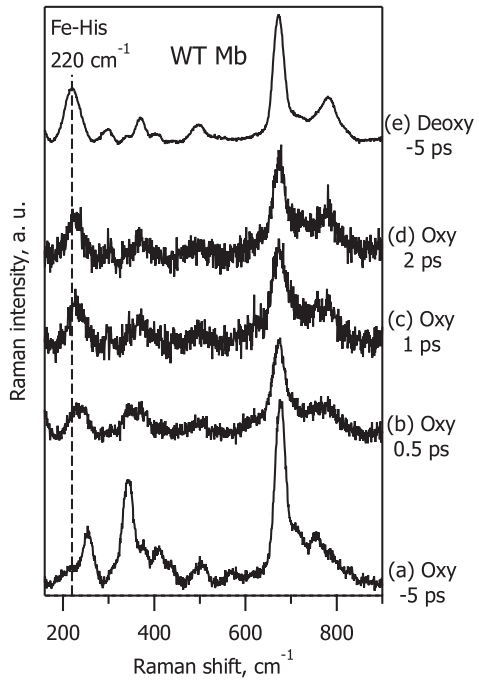

Fig. 4. TR^3 spectra in the low-frequency range of ferrous WT myoglobin, for the oxy complex (spectra a–d) and its deoxy form (spectrum e). Spectra a and e are ground-state spectra recorded at $\Delta t = -5$ ps. Spectra b–d are difference spectra at $\Delta t = 0.5$ps (spectrum b), 1 ps (spectrum c), and 2 ps (spectrum d).

To study in more detail the structure of the photoproduct of the oxy complex, we monitored the low-frequency range of the Raman spectrum and, in particular, the 200–250 cm^{-1} spectral region where the Fe-His band is expected to appear for five-coordinate domed heme structures (24). Fig. 3 compares TR^3 spectra in this range for WT FixLH in the oxy (spectra a–d), CO-bound (spectra e–h) and deoxy (spectrum i) forms. In the deoxy spectrum, the strong Fe-His band at 217 cm^{-1} is the dominating feature below 600 cm^{-1} (Fig. 3, spectrum i). This band is also clearly present in the difference spectra of the CO-bound complex at any time delay (Fig. 3, spectra f–h) revealing quasi-instantaneous CO ligand photodissociation and creation of the domed heme structure in a similar way as for MbCO (12, 14, 15). In striking contrast, TR^3 difference spectra of the FixLH oxy complex do not show any evidence of the Fe-His band, even at a time delay as short as 0.5 ps (Fig. 3, spectrum b).

To demonstrate that our experimental setup is sensitive enough to detect the 5cHS photoproduct of the heme oxy complex, we have investigated the low-frequency TR^3 spectra of MbO_2, for which the quantum yield of oxygen photodissociation was measured to be 28 ± 6%, from femtosecond transient absorption experiments (22). Fig. 4 shows that a strong Fe-His band appears immediately in the photoproduct spectra, revealing oxygen dissociation and subsequent heme doming for the oxymyoglobin transient species. The spectrum at $\Delta t = 2$ ps (Fig. 4, spectrum d) is very much deoxy-like (Fig. 4, spectrum e), in perfect agreement with expectation on the basis of previous transient absorption experiments (22, 30). At the same time, we note that the Fe-His band in dissociated MbO_2 experiences a progressive low-frequency shift from ≈225 cm^{-1} at $\Delta t = 0.5$ ps (Fig. 4, spectrum b) to ≈222 cm^{-1} at $\Delta t = 2$ ps (Fig. 4, spectrum d), which is still slightly shifted from the stationary deoxy-form value at 220 cm^{-1} (Fig. 4, spectrum e). This minor Fe-His band shift presumably reflects a gradual protein relaxation after oxygen ligand release from the heme; a similar effect was observed for MbCO after CO photodissociation (15).

From the comparison of the TR^3 difference spectra for oxy-FixLH (absence of Fe-His band; Fig. 3, spectra b–d) and oxymyoglobin (strong Fe-His band; Fig. 4, spectra b–d), we conclude that the 0.5-ps photoproduct heme structure is not domed in the case of oxy-FixLH.

To study the origin of this finding in more detail and, in particular, the role of arginine 220, we compared the behavior of WT FixLH with that of the R220H and R220Q mutant proteins. In WT FixLH-O_2, arginine 220 is hydrogen bonded to the terminal oxygen atom (Fig. 1). In FixLH-R220H-O_2, arginine is replaced by histidine, which is also hydrogen bonded to the terminal oxygen atom (8). In FixLH-R220Q-O_2, the terminal oxygen is not H bonded to the substituted glutamine, and instead the first oxygen atom that participates in axial ligation with the heme is H bonded (8).

Fig. 5 presents TR^3 spectra of FixLH-R220Q in the oxy (spectra a and b) and deoxy forms (spectrum c), as well as of FixLH-R220H in the oxy (spectra d and e), CO-bound (spectra f and g) and deoxy forms (spectrum h). Equilibration of the reduced FixLH-R220H mutant protein with 1 atm of O_2 (1 atm = 101.3 kPa) yields a 100% oxy complex, and its ground-state spectrum (Fig. 5, spectrum d) is consistent with the literature (8). It was previously reported that, upon oxygenation of the FixLH-R220Q mutant protein, ≈20% of the sample is in the deoxy form and that 80% is in the oxy form (8, 9). However,

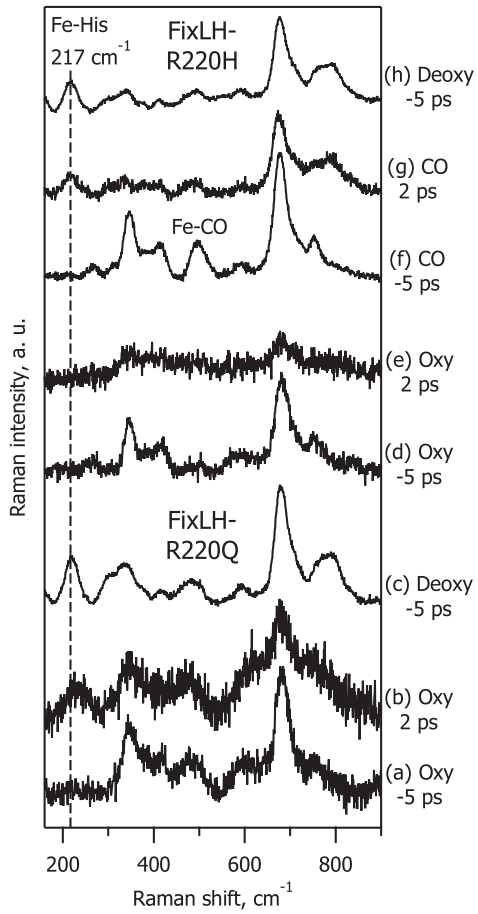

Fig. 5. TR^3 spectra in the low-frequency range of ferrous FixL mutants R220Q (spectra a–c) and R220H (spectra d–h), for their oxy (spectra a, b, d, and e), CO-bound (spectra f and g), and deoxy forms (spectra c and h). Spectra a, c, d, f, and h are ground-state spectra recorded at $\Delta t = -5$ ps. Spectra b, e, and g are difference spectra at $\Delta t = 2$ps.

under our present experimental conditions, no steady-state deoxy contribution was observed in oxygenated FixLH-R220Q, as revealed by the absence of an Fe-His band in the $\Delta t = -5$ ps spectrum (Fig. 5, spectrum a). We believe that the higher yield of the oxy complex is due to the efficient oxygenation of the sample under our experimental conditions (see *Methods*).

The TR^3 data show that the behavior of the FixLH-R220H mutant protein is similar to that of WT FixLH: No Fe-His band is observed for the oxy-photoproduct (Fig. 5, spectrum e), whereas a deoxy-like spectrum with a pronounced Fe-His band appears in the case of the CO photoproduct (Fig. 5, spectrum g). By contrast, in the oxy complex of the FixLH-R220Q mutant protein, we did observe the Fe-His band at $\Delta t = 2$ ps (Fig. 5, spectrum b), implying that a domed heme is formed, as in the case of oxymyoglobin (Fig. 4, spectrum d).

Finally, we note that for all proteins and ligands studied, weak and complex spectral changes occur as time elapses in the range of 250–450 cm^{-1}, which comprises the porphyrin in-plane modes ν_8 and ν_9, the porphyrin out-of-plane modes γ_6, γ_7, and γ_{16}, and the propionate $\delta(C_\beta C_c C_d)$ and vinyl $\delta(C_\beta C_a C_b)$ bending modes (31, 32). We cannot analyze these changes in detail because of insufficient spectral resolution, but in general, they reflect time-dependent changes in heme macrocycle conformation, as reported for allosteric transition in hemoglobin in refs. 33 and 34.

Discussion

TR^3 spectroscopy is a powerful technique to study transient heme structures after ligand photodissociation. Many previous TR^3 studies on heme proteins with external gaseous ligands have been limited essentially to CO (11–15), which acts as an inhibitor for most ligand-binding heme proteins. Such studies with the physiologically often more relevant oxy complexes are complicated because of the lower stability of these complexes and, at least for myoglobin, the lower apparent quantum yield of photodissociation (22). Here, we have succeeded in monitoring TR^3 spectra of oxymyoglobin and oxy-FixLH within the very first moments after photoexcitation with an instrument response of ≈0.7 ps. Importantly, for MbO_2, our results clearly demonstrate that upon dissociation of the physiological ligand O_2, a five-coordinate deoxy complex is formed faster than 0.5 ps (Fig. 4, spectrum b), in a very similar way as previously shown for dissociation of the inhibitor molecule CO from hemoglobin (12) and myoglobin (15).

For FixLH-O_2, contrary to MbO_2, our TR^3 data revealed that the photoproduct heme structure is not deoxy-like and is not domed at any time delay studied. What follows are the possible explanations for this finding considered in detail.

The experiments were based on the fact that the gaseous axial ligand can be dissociated from heme with a sizeable quantum yield (22, 30). As mentioned in the "Introduction," the hemes of myoglobin and FixL are chemically identical, share histidine as a proximal residue (as in the quasi-totality of heme proteins), coordinate to molecular oxygen in a very similar way, and display a very similar electronic absorption spectrum. This strongly suggests that the electronic structures of the ground and lowest excited states of the heme are nearly identical and that the excitation would lead to rupture of the heme-oxygen bond within tens of femtoseconds (35) with a similar yield. Also, we note that the efficiency of mixing of the excited state with the Fe-O_2 antibonding orbital is thought to be strongly determined by the bending configuration of the initially bound heme–ligand complex (22, 36). The remarkable similarity of the Fe-O-O angles in the oxy complex of MbO_2 (122 ± 1° from a 1.0 Å resolution structure; ref. 37) and FixLH-O_2 (124° from a 2.3 Å resolution structure; ref. 3) also point at near-identical intrinsic quantum yields of Fe-O_2 photoinduced bond breaking. In further support of this suggestion, we have also recorded transient absorption kinetics with 30-fs time resolution and found that the initial ground-state bleaching is similar for FixLH and Mb oxy complexes, but the following femtosecond relaxation is not [see supporting information (SI)].

Assuming a quantum yields of Fe-O_2 bond dissociation of FixLH close to that of Mb, as discussed above, in principle, on the basis of the observed TR^3 spectra at $t > 0.5$ ps, two possible scenarios can be considered to explain the FixLH photoproduct heme structure: (*i*) The oxygen-heme iron bond is broken and five-coordinate heme is formed, but the heme structure remains planar and there is no transition from low- to high-spin iron. (*ii*) The oxygen-heme iron bond is broken but the oxygen molecule is forced to stay in place by the environmental constraints and rebinds rapidly, preventing the creation of the deoxy-like domed heme structure.

The first assumption that the heme structure does not experience doming before oxygen recombination in ≈5 ps (time constant observed in transient absorption; ref. 7) seems unlikely. Indeed, in CO-dissociated hemoglobin and myoglobin heme, doming appears in <1 ps (12, 13), and in CO-dissociated FixL, the same is observed (Fig. 3, spectra f–h). Similar observations were made for the nitrosylated heme proteins cytochrome *c* (18), myoglobin-H93G (19), myoglobin, and FixL (S.G.K., A.J., and M.H.V., unpublished results), and for methionine photodissociation from ferrous cytochrome *c* (17, 20). For O_2-complexes, no TR^3 experiments have been published so far, but our present results show that in oxygen-dissociated Mb, doming occurs within 0.5 ps (Fig. 4, spectra b–d). These comparisons make it highly unlikely that steric constraints on the proximal side would

retain the heme in-plane upon dissociation of O_2 from FixL-O_2. In addition, the shifts of the ν_2^* and ν_4^* bands upon excitation of this complex (Fig. 2, spectrum c) are far less extensive than expected for a deoxy complex, revealing the absence of a low-to-high spin state transition in the photoproduct state.

Therefore, to explain our findings for oxy-FixLH, we propose that the rebinding of dissociated O_2 is mostly completed at 0.5 ps. In this view, the dissociated oxygen molecule cannot move away substantially from the heme because of steric constraints and remains in a favorable position for rebinding. This rebinding may then occur before or in competition with heme doming, which is expected to take ≈200 fs (the quarter period of the vibrational mode associated with iron out-of-plane motion, which is at ≈50 cm^{-1}; refs. 38–42). Theoretical studies on model systems have pointed at heme doming as an important parameter in determining the intrinsic affinity of heme for O_2 (43–45). Transient absorption experiments indeed show a recovery of the initially photobleached six-coordinate oxy complex in 80 fs in FixLH (see SI). A similar but less extensive recovery is observed in MbO_2, suggesting that the less-than-unity quantum yield on the picosecond timescale in both systems may originate from ultrafast recombination of O_2 and heme before doming.

In the previous transient absorption studies on FixLH-O_2 and DosH-O_2, we have reported a ≈5-ps decay component associated with a spectrum that is red-shifted with respect to the ground-state oxy-spectrum but far less than expected for a steady-state deoxy spectrum (7). This spectrum was assigned to a constrained oxygen-dissociated heme, and the present work was initiated to characterize this species. In view of our present TR^3 results, indicating a much faster heme–oxygen recombination, a reinterpretation of this feature is required. Most likely, it reflects cooling of a hot six-coordinate heme (20, 22, 46). Indeed, the observed ≈10 cm^{-1} downshifts of the ν_2^* and ν_4^* bands, with respect to the ground-state oxy complex, and the asymmetry of the ν_4^* band at $\Delta t = 2$ ps (Fig. 2, spectra b and c) are consistent with a vibrationally hot six-coordinate heme (*cf.* a similar analysis of ferric cytochrome *c* in ref. 20).

The previous estimate of ≈10% for the probability of dissociated O_2 to leave the immediate heme environment (7, 9) on the basis of the assignment in FixLH of the ≈5-ps phase to heme–O_2 recombination can also be reassessed. Measurements performed following the protocol of ref. 22 by using MbCO as a reference for unity quantum yield yielded a value of 5 ± 1% for the quantum yield of O_2 photodissociation on the time scale >5 ps. This very low yield is consistent with the concept of the FixL heme pocket acting as an oxygen trap, which we proposed in ref. 7, and implies that tracing the intermediates in the (oxy → deoxy) state transition in the single photon absorption regime is very challenging. This problem may be avoided by using longer and intense pump pulses, allowing numerous attempts to obtain a long-lived photodissociated state but at the price of strong heating of the protein due to absorption by the heme of multiple photons per net dissociation event. Generally, our results suggest that the overall low O_2 affinity of FixL (1) is determined essentially by the low probability of O_2 to penetrate the heme pocket for a configuration in which arginine 220 interacts with the heme (Fig. 1) rather than by the intrinsic heme–O_2 affinity.

Comparison of our TR^3 results on WT and mutant FixLH (Figs. 3 and 5) indicates that a hydrogen bond between the residue at position 220 (arginine in WT) and the terminal oxygen atom of the oxygen molecule (present in WT and R220H; ref. 8) plays an essential role in the steric constraints maintaining the oxygen molecule in place. The fact that doming is observed in the R220Q mutant, where Gln-220 makes a hydrogen bond with the iron-bound oxygen atom, but not with the terminal oxygen atom (8), correlates well with the relatively high yield of long-lived deoxy heme observed in ref. 9, and indicates that, in WT FixLH, it is through constraints on the terminal oxygen atom that O_2 is "pushed" toward the heme. Molecular dynamics simulations of the dissociated FixLH-O_2 complex also point at an essential role for Arg-220 in maintaining O_2 close to the heme (9).

In MbO_2, the terminal oxygen atom is also involved in H-bonding, interacting with the distal histidine (His 64) (47, 48), of similar strength as in the FixLH R220H mutant (8). As in MbO_2 substantial heme doming is observed (Fig. 5), in contrast to FixLH R220H, it is implied that this hydrogen bond is required, but not the only factor determining the high yield of fast O_2 recombination in FixLH. Different factors may also play a role. The Mb distal cavity harbors more polar residues than that of FixL and, assuming residual charges remain on O_2 shortly after dissociation, this may favor reorientation and migration out of the heme-binding configuration. Also, the free volume of motion appears larger in the Mb pocket than in the FixL pocket, as indicated by molecular dynamics simulations of dissociated oxygen (9, 49).

In summary, we have exploited high time resolution TR^3 spectroscopy to assess the heme structure after dissociation of oxygen from heme proteins. The surprising lack of appearance of an Fe-His mode in FixL indicates recombination of oxygen and heme on the 100-fs timescale, thus uncovering the origin of the "oxygen cage" properties of this oxygen sensor protein.

Materials and Methods

Sample Preparation. WT FixLH from *B. japonicum* and its R220H and R220Q mutants were prepared as described in refs. 7 and 8. Horse heart myoglobin was purchased from Sigma (St. Louis, MO). The proteins were prepared at a concentration of 100 μM in 50 mM Hepes buffer, pH 8.0. The sample (50–100 μl) was moved to the cylindrical 18-mm inner diameter cell (540.135, volume 14 ml; Hellma, Müllheim, Germany), equipped with a gastight seal of local design. The cell was spun at ≈10 Hz during the measurements. Because of the centrifugal formation of a thin sample layer, this arrangement allowed (*i*) the use of a minimal amount of sample for each measurement and (*ii*) efficient equilibration with the voluminous gas phase. The sample was reduced directly in the cell under the argon atmosphere, for deoxy and carboxy complexes with 10 mM sodium dithionite, and for oxy complexes with 20 mM sodium ascorbate (26,855-0; Aldrich, St. Louis, MO) [in some cases, 10–20 μM ruthenium hexaamine was added as a redox mediator (50) to assure rapid rereduction after autoxidation]. For carboxy complexes, the sample was equilibrated with 1 atm of CO.

For oxycomplexes, immediately before the measurement the sample was equilibrated with 1 atm of O_2, and each sample was used to accumulate a Raman signal for 5 min. After this time, the sample was changed to a fresh solution, because the appearance of a nonidentified fluorescent component, presumably catalyzed by heme autooxidation, started to deteriorate the signal-to-noise ratio for all oxy-heme proteins. It was verified by steady-state absorption spectroscopy that the heme remained for >95% in the ferrous-oxyform because of the presence of excess ascorbate under these conditions.

Subpicosecond Raman Spectroscopy. The Raman spectrometer, based on a 1-kHz Ti:Sapphire system, and using pump pulses centered at 560–580 nm and probe pulses at 435 nm (Gaussian instrument response function of 0.65 ± 0.06 ps FWHM; spectral resolution 30 cm^{-1}) has been outlined elsewhere (17, 19, 20, 23). In the present work, we fully exploited the temporal resolution of the system and performed measurements at a delay time (0.5 ps) in which pump and probe still somewhat temporally overlap. To minimize the cross-phase modulation artifact (which gives rise to de facto broadening of the Rayleigh scattering line), the maximum intensity of the pump pulse was diminished by lengthening it from <100 fs to ≈250 fs; this had minimal effect on the overall temporal resolution, which is essentially determined by

the length of the probe pulse. The pump pulse energy was 1.5–2.0 μJ, and the probe-pulse energy was 20–30 nJ in the sample cell. Pump and probe beams were collinearly superimposed by a dichroic mirror and focused by a spherical lens with $f = 10$ cm. Raman spectra were recorded using a 90° light-collection geometry with excitation from the bottom of the cell. The total signal acquisition time of each spectrum was 15–25 min.

Steady-State Resonance Raman Spectroscopy. Steady-state resonance Raman spectra were recorded by replacing the pulsed Raman excitation at 435 nm by a cw excitation from He-Cd laser at 441.6 nm. For deoxy FixLH and FixLH-O_2, variation of excitation power in the range of 0.5–5 mW did not affect the cw RR spectra (data not shown), whereas for FixLH-CO, power-induced transformations were evident. To record cw RR spectrum of six-coordinate FixLH-CO complex, excitation power of 0.45 mW was used that did not cause noticeable photoinduced spectral changes.

We thank Latifa Bouzhir-Sima for help in sample preparation and Tony Mattioli for stimulating discussions. S.G.K. was partially supported by fellowships from Fondation pour la Recherche Médicale, Institut National de la Santé et de la Recherche Médicale, and Ecole Polytechnique. A.J. was the recipient of a long-term fellowship from the European Molecular Biology Organization. K.H. was the recipient of an EC Marie Curie Training Site Fellowship. T.Y. is the recipient of a European Commission Marie Curie Incoming International Fellowship.

1. Gilles-Gonzalez MA, Gonzalez G, Perutz MF, Kiger L, Marden MC, Poyart C (1994) *Biochemistry* 33:8067–8073.
2. Tuckerman JR, Gonzalez G, Dioum EM, Gilles-Gonzalez MA (2002) *Biochemistry* 41:6170–6177.
3. Gong W, Hao B, Chan MK (2000) *Biochemistry* 39:3955–3962.
4. Hao B, Isaza C, Arndt J, Soltis M, Chan MK (2002) *Biochemistry* 41:12952–12958.
5. Dunham CM, Dioum EM, Tuckerman JR, Gonzalez G, Scott WG, Gilles-Gonzalez MA (2003) *Biochemistry* 42:7701–7708.
6. Rodgers KR, Lukat-Rodgers GS, Tang L (1999) *J Am Chem Soc* 121:11241–11242.
7. Liebl U, Bouzhir-Sima L, Négrerie M, Martin J-L, Vos MH (2002) *Proc Natl Acad Sci USA* 99:12771–12776.
8. Balland V, Bouzhir-Sima L, Kiger L, Marden MC, Vos MH, Liebl U, Mattioli TA (2005) *J Biol Chem* 280:15279–15288.
9. Jasaitis A, Hola K, Bouzhir-Sima L, Lambry J-C, Balland V, Vos MH, Liebl U (2006) *Biochemistry* 45:6018–6026.
10. Gilles-Gonzalez MA, Ditta GS, Helinski DR (1991) *Nature* 350:170–172.
11. Petrich JW, Martin J-L, Houde D, Poyart C, Orszag A (1987) *Biochemistry* 26:7914–7923.
12. Franzen S, Lambry JC, Bohn B, Poyart C, Martin J-L (1994) *Nat Struct Biol* 1:230–233.
13. Franzen S, Bohn B, Poyart C, Martin J-L (1995) *Biochemistry* 34:1224–1237.
14. Mizutani Y, Kitagawa T (1997) *Science* 278:443–446.
15. Mizutani Y, Kitagawa T (2001) *J Phys Chem B* 105:10992–10999.
16. Sato A, Sasakura Y, Sugiyama S, Sagami I, Shimizu T, Mizutani Y, Kitagawa T (2002) *J Biol Chem* 277:32650–32658.
17. Cianetti S, Négrerie M, Vos MH, Martin J-L, Kruglik SG (2004) *J Am Chem Soc* 126:13932–13933.
18. Cianetti S, Kruglik SG, Vos MH, Turpin PY, Martin J-L, Négrerie M (2004) *Biochim Biophys Acta* 1658:218.
19. Négrerie M, Kruglik SG, Lambry JC, Vos MH, Martin J-L, Franzen S (2006) *J Biol Chem* 281:10389–10398.
20. Négrerie M, Cianetti S, Vos MH, Martin J-L, Kruglik SG (2006) *J Phys Chem B* 110:12766–12781.
21. Antonini E, Brunori M (1971) *Hemoglobin and Myoglobin in Their Reactions with Ligands* (North–Holland, Amsterdam).
22. Ye X, Demidov A, Champion PM (2002) *J Am Chem Soc* 124:5914–5924.
23. Kruglik SG, Lambry JC, Cianetti S, Martin J-L, Eady RR, Andrew CR, Negrerie M (2007) *J Biol Chem* 282:5053–5062.
24. Kitagawa T (1988) in *Biological Applications of Raman Spectroscopy*, ed Spiro TG (Wiley, New York), Vol 3, pp 97–131.
25. Spiro TG, Li XY (1988) in *Biological Applications of Ramans Spectroscopy*, ed Spiro TG (Wiley, New York), Vol 3, pp 1–37.
26. Tamura K, Nakamura H, Tanaka Y, Oue S, Tsukamoto K, Nomura M, Tsuchiya T, Adachi S, Takahashi S, Iizuka T, Shiro Y (1996) *J Am Chem Soc* 118:9434–9435.
27. Tomita T, Gonzalez G, Chang AL, Ikeda-Saito M, Gilles-Gonzalez MA (2002) *Biochemistry* 41:4819–4826.
28. Balland V, Bouzhir-Sima L, Anxolabéhère-Mallart E, Boussac A, Vos MH, Liebl U, Mattioli TA (2006) *Biochemistry* 45:2072–2084.
29. Kruglik SG, Mojzes P, Mizutani Y, Kitagawa T, Turpin PY (2001) *J Phys Chem B* 105:5018–5031.
30. Petrich JW, Poyart C, Martin J-L (1988) *Biochemistry* 27:4049–4060.
31. Hu SZ, Morris IK, Singh JP, Smith KM, Spiro TG (1993) *J Am Chem Soc* 115:12446–12458.
32. Hu S, Smith KM, Spiro TG (1996) *J Am Chem Soc* 118:12638–12646.
33. Jayaraman V, Rodgers KR, Mukerji I, Spiro TG (1995) *Science* 269:1843–1848.
34. Jayaraman V, Spiro TG (1996) *Biospectroscopy* 2:311–316.
35. Martin J-L, Vos MH (1992) *Ann Rev BiophysBiomol Struct* 21:199–222.
36. Bersuker IB, Stavrov SS (1988) *Coord Chem Rev* 88:1–68.
37. Vojtchovský J, Chu K, Berendzen J, Sweet RM, Schlichting I (1999) *Biophys J* 77:2153–2174.
38. Srajer V, Reinisch L, Champion PM (1988) *J Am Chem Soc* 110:6656–6670.
39. Li XY, Zgierski MZ (1992) *Chem Phys Lett* 188:16–20.
40. Zhu L, Sage JT, Champion PM (1994) *Science* 266:629–632.
41. Klug DD, Zgierski MZ, Tse JS, Liu Z, Kincaid JR, Czarnecki K, Hemley RJ (2002) *Proc Natl Acad Sci USA* 99:12526–12530.
42. Rosca F, Kumar ATN, Ionascu D, Ye X, Demidov AA, Sjodin T, Wharton D, Barrick D, Sligar SG, Yonetani T, Champion PM (2002) *J Phys Chem A* 106:3540–3552.
43. Rovira C, Parrinello M (1998) *Int J Quantum Chem* 70:387–394.
44. Capece L, Marti MA, Crespo A, Doctorovich F, Estrin DA (2006) *J Am Chem Soc* 128:12455–12461.
45. Torrens F (2004) *J Incl Phenom Macrocyc Chem* 49:37–46.
46. Ye X, Demidov A, Rosca F, Wang W, Kumar A, Ionascu D, Zhu L, Barrick D, Wharton D, Champion PM (2003) *J Phys Chem A* 107:8156–8165.
47. Phillips SEV, Schoenborn BP (1981) *Nature* 292:81–82.
48. Springer BA, Sligar SG, Olson JS, Phillips GN, Jr (1994) *Chem Rev* 94:699–714.
49. Lambry J-C (1997) PhD thesis (University of Paris XI, Orsay, France).
50. Brunori M, Giuffre A, D'Itri E, Sarti P (1997) *J Biol Chem* 272:19870–19874.